Tellus
SERIES B
CHEMICAL
AND PHYSICAL
METEOROLOGY
PUBLISHED BY THE INTERNATIONAL METEOROLOGICAL INSTITUTE IN STOCKHOLM

The SAMUM-1 experiment over Southern Morocco: overview and introduction

By JOST HEINTZENBERG*, *Leibniz Institute for Tropospheric Research (IfT), Permoserstr. 15, 04318 Leipzig, Germany*

ABSTRACT

In May/June 2006, the largest mineral dust experiment to date (Saharan Mineral Dust Experiment, SAMUM-1) was conducted in Southern Morocco. The aim was to characterize dust particles near the world's largest mineral dust source, and to quantify dust-related radiative effects. At one of the two ground-based measurement sites dust particle size distribution, optical, hygroscopic, chemical and structural particle characteristics were measured. One research aircraft mainly measured solar spectral irradiances and surface albedo. The other aircraft provided in situ physical aerosol measurements and samples and lidar profiles through the dust layers. Three ground-based lidars were operated at the second ground-based measurement site. They determined optical dust properties, particle shape and temporal development of dust layers. Columnar, ground-based sun photometer measurements complemented the lidar data. Additionally a station in Évora, Portugal monitored dust outbreaks from the North African source region to the Iberian Peninsula during SAMUM-1.

Volumetric and columnar closure exercises utilized these detailed measurements of dust characteristics together with optical and radiative transfer models. Concurrent developments of a mesoscale dust transport model were validated with the experimental data. The paper gives an overview over rationale and design of SAMUM-1, introduces and highlights the subsequent reports on experimental and modelling results.

1. Introduction

In 2007, the Intergovernmental Panel on Climate Change (IPCC) published its fourth report (4AR, IPCC, 2007). Another 6 yr of Earth system research had passed since the third IPCC report (TAR, Houghton et al., 2001) but the uncertainties of the projected temperature change had not decreased. One of the few main factors for this apparent lack of progress is the multi-faceted atmospheric aerosol of which many characteristics are incompletely established and many processes not yet fully understood. The largest natural source of particulate aerosol mass is mineral dust from dry continental regions. Estimates of the global source strength of dust particles, however, vary between 1000 and 5000 Tg yr^{-1} (Duce, 1995; Prospero et al., 2002; Cakmur et al., 2006). In 2001, TAR reported a global change in radiative balance at the top of the atmosphere (TOA) (radiative forcing, RF) due to anthropogenic mineral dust in the range of +0.4 to −0.6 W m^{-2}, and did not assign a best estimate because of the difficulties in determining the anthropogenic contribution

to the total dust loading and the uncertainties in the optical properties of dust and in evaluating the competing short-wave and long-wave radiative effects. In 4AR, the revised anthropogenic contribution to dust direct RF of at most 20% (Tegen et al., 2004) and the revised absorption properties of dust yielded a small negative value for the anthropogenic direct RF for dust of −0.1 ± 0.2 W m^{-2}. This small estimate of anthropogenic direct dust effect on Earth's energy balance conceals a substantial redistribution of energy from the surface to the often several kilometres deep dust layers with significant feedbacks and responses of the Earth system. Thus, the global impact of total dust on the Earth system still remains highly uncertain.

The Sahara is the largest source region of mineral dust. Besides a major influence on the energy distribution in the Earth/atmosphere system, the Sahara fertilizes the Atlantic phytoplankton (Jickells et al., 2005) and the Amazonian rain forest (e.g. Koren et al., 2006). There are papers suggesting that Saharan dust interferes with the formation of tropical cyclones in the Caribbean hurricane alley (e.g. Evan et al., 2006; Lau and Kim, 2007; Wu, 2007).

The direct radiative effects caused by mineral dust are complex, since dust particles not only scatter but also partly absorb incoming solar radiation, and the dust particles absorb and emit

*Corresponding author.
e-mail: jost@tropos.de

outgoing long-wave radiation. The magnitude and even the sign of the net (i.e. solar plus long wave) dust RF depend on the optical properties of the dust, its vertical distribution, the presence of clouds and on the albedo of the underlying surface (Sokolik and Toon, 1996; Tegen et al., 1996; Liao and Seinfeld, 1998; Myhre and Stordal, 2001). A prerequisite for estimating the radiative effects and interactions of dust and climate is the quantification of atmospheric dust loads and size-dependent optical properties of the dust particles. Large-scale dust distributions can be retrieved from satellite data, although over highly reflective surfaces like most deserts these retrievals so far are mostly just qualitative. This is because of uncertainties in the a priori assumptions about aerosol optical properties (e.g. Sokolik et al., 2001) and considerable uncertainties related to the surface reflection.

The limited number of existing measurements of dust particle properties is neither sufficient to constrain realistic estimates of dust loads, which are highly variable in space and time nor to model dust effects on radiation balance, weather and climate. A comprehensive field investigation of mineral dust close to a major source region with minimum influence of anthropogenic, biogenic or marine aerosol sources has not been conducted to date. Therefore, a consortium of six German research groups conceived the Saharan Mineral Dust Experiment (SAMUM)-project combining their competence in field experiments, satellite retrievals and model developments. The first 3-yr phase (2004–2006) concentrated on physical dust characteristics and effects on the energy balance near its source culminating in the SAMUM-1 field experiment in May/June 2006 in Southern Morocco. Two heavily instrumented ground-based stations and two research aircraft were operated during the experiment. The present special issue focuses on results of SAMUM-1 and concurrent modelling efforts. A SAMUM-2 experiment in the Saharan dust plum over the Atlantic was conducted over the Cape Verde Islands in January/February 2008.

2. Design of the SAMUM-1 experiment

Large-scale effects of mineral dust on energy balance and climate can only be assessed through numerical models with sufficient coverage, resolution and physical completeness. They need to be constrained by detailed physical dust characteristics, in particular spectral optical properties of the dust particles (in particular their size and single-scattering albedo). Consequently, a large part of the experimental efforts was dedicated to a detailed physical characterization of the dust particles.

Model validation requires high-resolution physical dust and radiation data throughout the dust-filled part of the atmosphere. Previous dust experiments mostly focused on either ground-based or airborne measurements, whereas SAMUM-1, for the first time, combined collocated and simultaneous state-of-the-art ground-based aerosol characterization, ground-based and airborne aerosol and radiation profiling plus satellite data.

Internal consistency and realistic assessments of uncertainties in volumetric[1] dust measurements as well as throughout atmospheric columns are essential in the evaluation of atmospheric aerosol experiments. For that purpose, SAMUM-1 followed the closure approach which Ogren (1995) developed, and Quinn et al. (1996) extended. Ansmann et al. (2002), Russell and Heintzenberg (2000) and others had tested this approach in aerosol field experiments but never in an aerosol source region dominated by mineral dust.

Global characteristics of the atmospheric aerosol can only be monitored from space. However, the related techniques for the retrieval of aerosol parameters require validation for which the data collected during SAMUM-1 offer a unique opportunity. In the common passive remote sensing of reflected solar radiation, and in particular over highly reflective desert source regions of dust, most of the signal received by satellite radiometers is due to surface reflection. Thus, measurements of spectral surface albedo in the working area of SAMUM-1 became an important component of the programme.

As a compromise between the scientific demand of closeness to the dust sources and logistic and political compromises the consortium chose Southern Morocco as the working area of SAMUM-1. Most of the experiment was concentrated at the two ground stations Ouarzazate (30.9°N, 6.9°W, 1133 m height above sea level, asl) and Tinfou near Zagora (30.24°N and 5.61°W about 730 m asl), while the larger of the two research aircrafts (Falcon, DLR) operated out of Casablanca.

2.1. Modelling efforts

In Fig. 1, the locations of the SAMUM-1 sites are depicted together with the modelled field of aerosol optical depth (AOD) at 550 nm wavelength during a strong dust outbreak. This figure also shows the associated station of the University of Évora (38.57°N, 7.91°W, 293 m asl), which measured dust outbreaks from North Africa. Regional dust distributions were simulated for the SAMUM-1 period with the regional dust model system LM-MUSCAT (Heinold et al., cf. Table 3). Simulations were performed for the period from 9 May to 5 June 2006. Dust emission, transport and deposition are computed for five independent size classes using meteorological and hydrological fields provided by the non-hydrostatic operational weather prediction model Consortium for Small-scale Modelling (COSMO) of the German weather service (DWD). The model domain covers major parts of the Sahara desert and Southern Europe. For simulations of the dust episodes during the SAMUM campaign shown in Fig. 1, a horizontal resolution of 28 km is used for the area between 13.86°N, 25.35°W and 47.78°N, 38.16°E. The model is operated with 40 vertical layers of a terrain-following vertical coordinate. The simulation of dust emissions takes into account

---

[1]Volumetric in the sense of related to the aerosol particles in a small sensing or sampling volume of air.
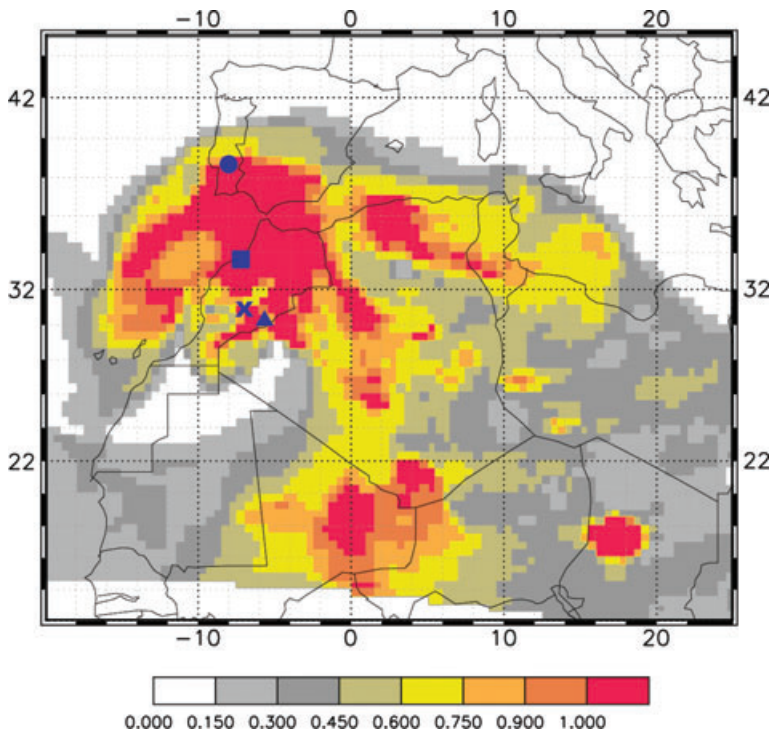
Fig. 1. The coloured map (longitude, latitude north in degrees) shows dust distribution modelled by Heinold et al. (cf. Table 3) in terms of aerosol optical depth (AOD) at 550 nm wavelength during a strong dust outbreak on 27 May 2006 12 UTC. The four SAMUM-1 sites Casablanca, Ouarzazate, Zagora and Évora are indicated by a blue square, cross, triangle and circle, respectively.

soil properties like texture and surface roughness, and prescribes enclosed topographic depressions as preferential dust emission sources. Dust is removed from the atmosphere by dry and wet deposition processes. Dust optical thicknesses are computed from the simulated dust concentrations, particle size distribution and extinction efficiencies.

2.2. Experimental

The research aircraft Falcon of the German Aerospace Center (DLR) probed the entire tropospheric column from 10 km asl down to 500 m above ground and measured horizontal sections of the vertical dust distribution. The Falcon in situ instrumentation consisted of aerosol sizing instruments with and without thermodenuder upstream. Aerosol absorption was measured at three wavelengths in the visible spectral region. A nadir-looking high spectral resolution lidar (HSRL) measured atmospheric backscatter, particulate extinction and linear depolarization including molecular backscatter. Dust samples were collected in flight for subsequent laboratory analyses.

At the airport of Ouarzazate, the smaller aircraft Partenavia (IfT) was stationed. This aircraft, operated by 'enviscope GmbH', was mainly used to measure spectral solar upwelling and downwelling spectral irradiance and actinic flux densities from which the spectral surface albedo was derived and to probe the boundary layer in the vicinity of the two field sites. At the same time impactor samples of particles in the dust layers were taken for subsequent laboratory analyses.

Three polarization-Raman lidar systems, two of the University of Munich (LMU) and a large one of IfT were set up at the airport. This unique lidar-park measured backscatter coefficients at six wavelengths from 355 to 1064 nm while extinction coefficients at 355 and 532 nm were recorded. The derived extinction-to-backscatter ratios (at 355, 532 and 1064 nm) together with depolarization of the backscattered radiation measured at four wavelengths proved of particular value when characterizing layers of highly non-spherical dust particles.

Additionally, an NASA Aerosol Robotic Network (AERONET, Holben et al., 1998) sun photometer operated by IfT measured AODs from 380 to 1640 nm wavelength. University of Munich operated the Sun–sky automatic radiometer (SSARA), a similar instrument covering the spectral range from 339 to 1553 nm. Both radiometers measured sky radiances at selected wavelengths as well. A radiosonde station operated by IfT complemented the Ouarzazate station. Table 1 summarizes the remotely sensed aerosol optical parameters and radiation measurements.

Some 120 km southeast of Ouarzazate near the town Zagora most of the volumetric in situ instrumentation and aerosol sampling was set up in and on a container laboratory within the premises of the Kashba Hotel Porte au Sahara. A host of methods operated by groups of IfT and the Universities of Darmstadt and Mainz measured particle size distributions covering the size range of 20 nm to 500 μm. Mass concentrations in three size classes were evaluated gravimetrically from filter samples. The laboratory of Darmstadt University determined elemental and mineral particle composition on bulk and size-segregated

Table 1. Remotely sensed dust parameters, related instrumentation data, platforms and methodological papers in this issue

Parameter	Instrument	Platform or site	Wavelengths (nm)	Laboratory	Method paper in this issue
Backscatter coefficient	High spectral resolution lidar (HSRL)	Falcon	532, 1064	DLR-PA	Esselborn et al.
Extinction coefficient	HSRL	Falcon	532	DLR-PA	Esselborn et al.
Depolarization	HSRL	Falcon	532, 1064	DLR-PA	Esselborn et al.
Irradiances and actinic flux densities	Spectral modular airborne radiation measurement system (SMART)-albedometer	Partenavia	290–2200	IfT	Bierwirth et al.
Backscatter coefficient	Lidar-POLIS	Ouarzazate, Zagora	355	LMU	Freudenthaler et al., Heese et al.
Extinction coefficient	Lidar-POLIS	Ouarzazate, Zagora	355	LMU	Freudenthaler et al., Heese et al.
Depolarization	Lidar-POLIS	Ouarzazate, Zagora	355	LMU	Freudenthaler et al., Heese et al.
Backscatter coefficient	Lidar-MULIS	Ouarzazate	355, 532	LMU	Freudenthaler et al.
Extinction coefficient	Lidar-MULIS	Ouarzazate	355	LMU	Freudenthaler et al.
Depolarization	Lidar-MULIS	Ouarzazate	532	LMU	Freudenthaler et al.
Backscatter coefficient	Lidar-BERTHA	Ouarzazate	355, 400, 532, 710, 800, 1064	IfT	Tesche et al.
Extinction coefficient	Lidar-BERTHA	Ouarzazate	355,532	IfT	Tesche et al.
Depolarization	Lidar-BERTHA	Ouarzazate	710	IfT	Tesche et al.
Aerosol optical depth, phase function	AERONET sun photometer	Ouarzazate	380–1640	IfT	Tesche et al.
Aerosol optical depth, phase function	Sun–sky automatic radiometer (SSARA)	Ouarzazate	339–1552	LMU	Toledano et al.
Downwelling irradiance	Compact radiation measurement system (CORAS)	Ouarzazate	280–1050	IfT/UMz	Bierwirth et al.
Downwelling actinic flux density	Compact radiation measurement system (CORAS)	Ouarzazate	280–1050	IfT/UMz	Bierwirth et al.
Downwelling and upwelling broad-band long-wave radiation	Compact radiation measurement system (CORAS)	Ouarzazate	4000–42000	IfT/UMz	Bierwirth et al.
Aerosol optical depth, phase function	CIMEL CE 318 sun photometer	Zagora	340–1020	UBr	Hoyningen-Huene et al.

Note: DLR-PA, German Aerospace Research Center, Institute for Physics of the Atmosphere; LMU, Meteorological Institute, Ludwig-Maximilians-Universität, München; Umz, Institute for Physics of the Atmosphere, Johannes-Gutenberg-Universität Mainz; Ubr, Institute for Environmental Physics, University of Bremen.
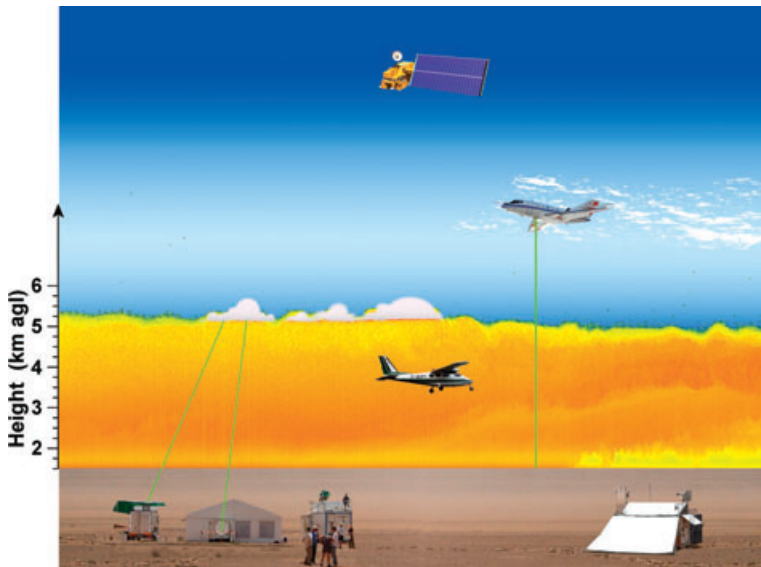
Fig. 2. Schematic overview of the SAMUM-1 experiment with the MISR satellite system, Falcon, and Partenavia aircraft (top to bottom), lidar station at Ouarzazate airport (left-hand side), and Zagora station (right-hand side). The dust layer reaching up to 5 km (cf. left scale) is visualized by a measured lidar backscatter time/height profile.

samples. With particle hygroscopicity determined by IfT over a wide range of particle sizes ambient optical dust properties can be adjusted to varying relative humidities. IfT determined spectral light scattering and absorption by dust particles in airborne and in deposited state. For a limited time period one of the two LMU-lidars was moved to Zagora for comparative aerosol profiling. An overview of the complete experimental set up is given in Fig. 2 and Table 2 summarizes the volumetric dust measurements and sample analyses.

3. Highlights

3.1. *Measurements*

This special issue comprises the articles listed in Table 3, presenting results of the SAMUM-1 experiment, accompanying model work and meteorological analyses. The latter are introduced by Knippertz et al.,[2] who discuss differential advection of air masses with different characteristics during stable nighttime conditions and up to 5-km deep vertical mixing of dust in the strongly convective planetary boundary layer during the day. Their Lagrangian and synoptic analyses of selected dust periods point to a topographic channel from western Tunisia to central Algeria as an important source region for mineral dust. Significant emission events were traced to cold surges from the Mediterranean in association with the eastward passage of an upper-level wave and lee cyclogenesis south of the Atlas Mountains. Local emissions under a cut-off low over northwestern Africa and gust fronts associated with dry thunderstorms over the Malian and Algerian Sahara were other relevant events for SAMUM-1.

At the Zagora station number concentrations up to 1000 cm^{-3} and mass concentrations ranging up to 300 000 μg m^{-3} for total suspended particulate matter during moderate dust storms were measured. Even at the far-field site of SAMUM-1 in Southern Portugal mass concentrations of to 150 μg m^{-3} were recorded during a strong dust outbreak (Wagner et al.). Size distributions were measured and parametrized (Kaaden et al.; Kandler et al. and Schladitz et al.) for particles between 20 nm and 500 μm diameter. They could distinguish two major regimes of the size distribution. The submicrometer maxima around 80 nm were largely unaffected by varying meteorological and dust emission conditions. Above 500 nm, concentrations varied up to one order of magnitude, and up to three orders of magnitude above 10 μm.

Size-dependent hygroscopic growth properties of Saharan dust were measured by Kaaden et al. up to 85% relative humidity (RH) to relate physical, in particular optical, particle properties to their effects at ambient conditions. For the radiative properties (in particular scattering) of mineral dust particles, shape is an important factor that needs to be considered. For the particle number size distribution, a size-dependent shape factor was derived by Schladitz et al. This factor ranged from 1 at a particle diameter of 300 nm to 1.26 for supermicrometer particles (Kaaden et al.). As related parameter, the aspect ratio was measured by Kandler et al. Its size-dependence reflected particle composition with a rather constant aspect ratio of 1.6 for particles >500 nm diameter decreasing to about 1.3 for smaller sizes.

Kandler et al. also determined the mineralogical composition of bulk particle samples. Major compounds of the aerosol were quartz, potassium, feldspar, plagioclase, calcite, haematite and the clay minerals illite, kaolinite and chlorite. Only a small temporal variability of the bulk mineralogical composition was encountered. Microscopic single particle analysis yielded three

---

[2]All undated citations refer to Table 3.

Table 2. Dust parameters derived from in situ measurements and samples, related instrumentation data, platforms and methodological papers in this issue

Parameter	Instrument/analysis	Platform or site	Particle diameters	Wavelengths (nm)	Laboratory	Method paper in this issue
Particle number size distribution	Condensation particle counters + optical particle counters	Falcon	4 nm–100 μm		DLR-PA	Weinzierl et al.
Volatile number fraction	Thermodenudert + diffusion screens + condensation particle counters + optical particle counters	Falcon	4 nm–2.5 μm		DLR-PA	Weinzierl et al.
Absorption coefficient	Particulate absorption photometer	Falcon	4 nm–2.5 μm	467, 530, 660	DLR-PA	Petzold et al.
Single particle composition and morphology, refractive index	Impactor + SEM + EDX single particle analysis	Falcon	700 nm–4 μm		UDa	Kandler et al.
Single particle composition and morphology, refractive index	Impactor + SEM + EDX single particle analysis	Partenavia	700 nm–50 μm		UDa	Kandler et al.
Particle number size distribution	Differential mobility analyser	Zagora	20–800 nm		IfT	Schladitz et al.
Particle number size distribution	Aerodynamic particle spectrometer	Zagora	800 nm–10 μm		IfT	Schladitz et al.
Particle number size distribution	Free rotating wing impactor + single stage impactor	Zagora	4 μm–500 μm		UMz	Kandler et al.
Particle hygroscopicity	Hygroscopic tandem differential mobility analyser	Zagora	30–350 nm		IfT	Kaaden et al.
Particle hygroscopicity	High-flow-differential mobility analyser + humidified aerodynamic particle sflopectrometer	Zagora	720–960 nm		IfT	Kaaden et al.
Particulate mass concentrations	Filter gravimetry	Zagora	Total, <10 μm, <2.5 μm		UMz	Kandler et al.
Mineral phase	X-ray diffractometry	Zagora	Total, <10 μm, <2.5 μm, impactor samples		UDa	Kandler et al.
Single particle composition and morphology, refractive index	Impactor + size-resolved single particle analysis	Zagora	150 -250 μm		UDa	Kandler et al.
Scattering and hemispheric backscattering coefficients	Integrating nephelometer	Zagora	<10 μm	450, 550, 700	IfT	Schladitz et al.
Absorption coefficient	Particle soot absorption photometer	Zagora	<10 μm	537	IfT	Schladitz et al.
Absorption coefficient	Multi-angle absorption photometer	Zagora	<10 μm	637	IfT	Schladitz et al.
Absorption spectra	Spectral particulate absorption photometer	Zagora	<10 μm	300–800	IfT	Müller, Th. et al
Visibility	Forward scattering photometer	Zagora		880	IfT	Müller, Th. et al.

Note: DLR-PA, German Aerospace Research Center, Institute for Physics of the Atmosphere; Uda, Institute for Appl. Geosciences, Darmstadt University of Technology; Umz, Institute for Physics of the Atmosphere, Johannes-Gutenberg-Universität Mainz.

Table 3. SAMUM-1 manuscripts of the special issue of Tellus B

Authors	Title
Ansmann et al.	Vertical profiling of convective dust plumes in Southern Morocco during SAMUM
Bierwirth et al.	Spectral surface albedo over Morocco and its impact on the radiative forcing of Saharan dust
Dinter et al.	Retrieval of aerosol optical thickness for desert conditions using MERIS observations during the SAMUM campaign
Diouri et al.	Columnar particle size distributions obtained during SAMUM experimental campaign in Southeast Morocco
Esselborn et al.	Spatial distribution and optical properties of Saharan dust observed by airborne high spectral resolution lidar during SAMUM 2006
Freudenthaler et al.	Depolarization-ratio profiling at several wavelengths in pure Saharan dust during SAMUM 2006
Heinold et al.	Regional Saharan dust modelling during the SAMUM 2006 Campaign
Heese et al.	Vertically resolved dust pptical properties during SAMUM: Tinfou compared to Ouarzazate
Hoyningen-Huene et al.	Measurements of desert dust optical characteristics at Porte au Sahara during SAMUM
Kaaden et al.	Mixing state and hygroscopic growth of Saharan dust
Kahn et al.	Desert dust air mass mapping in the Western Sahara, using particle properties derived from space-based multi-angle imaging
Kandler et al.	Size distribution, mass concentration, chemical and mineralogical composition, and derived optical parameters of the boundary layer aerosol at Tinfou, Morocco, during SAMUM 2006
Knippertz et al.	Dust mobilization and transport in the Northern Sahara during SAMUM 2006—a meteorological overview
Müller, D. et al.	EARLINET observations of the 14–22 May long-range dust transport event during SAMUM 2006: validation of results from dust transport modelling
Müller, Th. et al.	Spectral absorption coefficients and imaginary parts of refractive indices of Saharan dust during SAMUM-1
Otto et al.	Radiative closure of a Saharan dust plume observed during SAMUM
Petzold et al.	Saharan dust absorption and refractive index from aircraft-based observations during SAMUM 2006
Schladitz et al.	In situ measurements of optical properties at Tinfou (Morocco) during the Saharan Mineral Dust Experiment SAMUM 2006
Tesche et al.	Vertical profiling of Saharan dust with Raman lidars and airborne HSRL in Southern Morocco during SAMUM
Toledano et al.	Spectral aerosol optical depth characterization of desert dust during SAMUM 2006
Wagner et al.	Properties of dust aerosol particles transported to Portugal from the Sahara desert
Weinzierl et al.	Airborne measurements of dust layer properties, particle size distribution and mixing state of Saharan dust during SAMUM 2006
Wiegner et al.	Numerical simulations of optical properties of Saharan dust aerosols with emphasis on lidar applications

size regimes: Particles below 500 nm diameter mainly contained sulphates and mineral components. Particles with diameters between 500 nm and 50 μm, mainly contained silicates, and – to a lesser extent – carbonates and quartz. Above 50 μm diameter, approximately half of the particles consisted of quartz.

A major task of the volumetric experiments concerned the optical particle properties. Three different approaches utilizing light scattering and absorption data from the ultraviolet to the near infrared combined with size distribution and particle composition yielded consistent size-dependent complex refractive indices by Kandler et al., Müller, Th. et al. and Schladitz et al. With measured high-resolution absorption spectra the refractive indices were corrected for soot due to local combustion sources (Müller, Th. et al.).

Three-dimensional dust optical and radiation characteristics were sensed remotely with the three ground-based Raman lidars (Tesche et al.) and the HSRL on the Falcon (Esselborn et al.). A height-resolved statistical analysis revealed that the dust layer typically reached 4–6 km asl, sometimes even 7 km. A vertically inhomogeneous dust plume with internal dust layers was usually observed in the morning before the evolution of the boundary

layer started. By the early evening then the Saharan dust layer was well mixed. The dust AOD at 500 nm wavelength ranged from 0.2 to 0.8, Ångström exponents were between 0 and 0.4. The volume extinction coefficients at 355–532 nm wavelength varied from 30 to 300 Mm^{-1} with a mean value of 100 Mm^{-1} in the lowest 4 km asl. On average, extinction-to-backscatter ratios of 53–55 sr were obtained for all three laser wavelengths (355, 532 and 1064 nm). With a mobile lidar and with the airborne lidar, the optical dust characteristics and profiles at the central Ouarzazate station were connected with the results at the Zagora station (Weinzierl et al.). Over the Portugal station Wagner et al. measured AODs up to 0.53 in the dust outbreak with lidar ratios between 45 and 50 sr.

For the first time vertical profiles of the linear particle depolarization ratio δ^p of dust were determined at four wavelengths (cf. Table 1, Freudenthaler et al.). A mean δ^p at 532 nm of 0.31 was found with a negative correlation of δ^p with Ångström exponent. Even during periods with aerosol optical thickness ≤ 0.1 δ^p-values between 0.21 and 0.25 were measured. Wiegner et al. compared these depolarization measurements with results from scattering theory based on the *T*-matrix method using in situ

measurements—size distribution, shape distribution and refractive index as input parameters; particle shape was approximated by spheroids. The simulated values of δ^p were in the range of the measurements. A strict validation was not possible as too many microphysical parameters influence the lidar ratio and δ^p that could not be measured with the required accuracy.

Multiwavelength sun photometry complemented the lidar measurements. Toledano et al. measured AODs at Ouarzazate while Diouri et al. and Hoyningen-Huene et al. measured spectral AODs and sky brightness at the Zagora station. From the latter measurements columnar scattering phase functions of the particles were derived, which Dinter et al. and Kahn et al. utilized in validation of the retrieval algorithms for the satellite overpasses.

Esselborn et al. observed significant horizontal variability of the AOD by the airborne dust profiling south of the High Atlas Mountain range even in cases of a well-mixed dust layer. High vertical variations of the dust lidar ratio of 38–50 sr were observed in cases of stratified dust layers. The variability of the lidar ratio was attributed to dust advection from different source regions. The aerosol depolarization ratio was very similar to that from the ground-based lidars and showed only marginal vertical variations. Over the whole SAMUM-1 working region, the dust layers were found to range from ground up to 4–6 km asl. As observed on the Falcon, the dust particles exhibited two size regimes with different state of mixings: below 500 nm, the particles had a non-volatile core and a volatile coating. Larger particles consisted of non-volatile components only and contained some absorbing material. The real part of the dust refractive index was found almost constant with values close to 1.55. The imaginary part varied between blue and red wavelengths by a factor of 3–10, depending on the dust source region. Resulting single-scattering albedo values calculated from dust size distributions and refractive indices by means of Mie theory were 0.70–0.90 at 450 nm and 0.83–0.99 at 700 nm.

From airborne radiation measurements on the Partenavia aircraft, Bierwirth et al. derived the spectral surface albedo and dust RFs. These are the first airborne and spectral surface albedo data collected over bright desert surfaces over a larger terrain. They showed that the surface albedo has a major impact on the short-wave RF of Saharan dust. As derived from the measured albedo spectra, that the TOA short-wave RF changed by 12 W m^{-2} per 0.1 surface albedo change. The net (short wave plus long wave) TOA RF varied between -19 and $+24$ W m^{-2} for a surface albedo of 0.0 and 0.32, respectively. Over the bright surfaces of Southeast Morocco, the Saharan dust consequently always had a warming effect.

With different model assumptions concerning the non-sphericity of the dust particles and SAMUM-1 measured particle and surface properties Otto et al. explored the effects of particle shape on the energy balance. They simulated the downward radiative transfer to be less affected by the non-sphericity, but the upwelling was strongly influenced. Compared to Mie theory the non-sphericity could lead to enhanced short-wave cooling of the Earth/atmosphere system by up to a factor of 2.8.

Optical surface, profiling and columnar data were used to validate aerosol amount and type retrieved from multi-angle imaging spectroradiometer (MISR) observations, and to place the suborbital aerosol measurements into the satellite's larger regional context. On three moderately dusty days for which co-incident observations were made, MISR mid-visible aerosol optical thickness agreed with field measurements point-by-point to within 0.05–0.1. This is about as well as can be expected given spatial sampling differences; the space-based observations capture aerosol trends and variability over an extended region.

3.2. Model results

Heinold et al. used the experimental data in large-scale dust transport modelling with the regional dust model system LM-MUSCAT-DES. The performance of this system was evaluated for two time periods in May and June 2006. Dust optical thicknesses, number size distributions and the position of the maximum dust extinction in the vertical profiles agreed well with the observations. However, the spatio-temporal evolution of the dust plumes was not always reproduced due to inaccuracies in the dust source placement by the model. Whereas simulated winds and dust distributions were well matched for dust events caused by dry synoptic-scale dynamics, they were often misrepresented when dust emissions were caused by moist convection or influenced by small-scale topography that was not resolved by the model.

3.3. Unexpected findings

Serendipity is not a guiding concept in atmospheric fieldwork. However, with reliable and sensitive instruments directed with an open mind at the complex atmospheric multiphase system chances are good for interesting unexpected results. In the case of SAMUM-1, two such unplanned for or unexpected results are reported.

The first set of findings of this character concerned dust mobilization mechanisms. Local emissions in the form of dust devils were readily observed for the first time by (but also a nuisance to) the lidars systems. For 5 d with favourable conditions for convective activity Ansmann et al. provide detailed statistics in form of frequency, height and meteorological conditions. Knippertz et al. (2007) discuss another relevant local dust mobilization mechanism for SAMUM-1, that is, density currents driven by the evaporation of precipitation over the Atlas Mountains. Despite the vigorous vertical mixing in the strongly convective boundary layer, some distinct emission events could be identified in the mineralogical composition and optical properties of dust sampled over Southern Morocco (Kandler et al.; Knippertz et al. and Petzold et al.).

The lidar system also yielded a second and unexpected result because of the frequent occurrence of altocumulus imbedded in or near the top of deep dust layers. Surprisingly, most of the altocumulus clouds that formed about the top of the Saharan dust layer, which reached into heights of 4–7 km asl and had layer top temperatures of -8 to $-18\,°C$, did not show any ice formation. According to the lidar observations by Ansmann et al. (2008), cloud top temperatures typically had to reach values as low as $-20\,°C$ before measurable ice formation started (which is lower than conventional knowledge).

4. Conclusions

In May/June 2006, a comprehensive mineral dust experiment SAMUM-1, with state-of-the-art instrumentation, was conducted over Southeast Morocco to characterize all relevant physical properties and optical effects of the Saharan mineral dust aerosol close to its source in terms of volumetric characteristics and in columnar properties and profiles from the surface to the TOA. The final goal of SAMUM-1 is to improve the accuracy on the calculation of regional and global RF of mineral dust.

During the experiment the aerosol varied from very low turbidity, associated with Atlantic air masses, to moderate, and high dust loads, in air masses arriving from Northern and West Saharan source regions. Dusty conditions were predominant during SAMUM-1 (78% of data), with AODs at 500 nm ≥ 0.15 with maxima about 0.8 and Ångström exponents ≤ 0.4. Dry particle single-scattering albedo values ranged from 0.7 to 0.99 depending on wavelength and extent of anthropogenic soot fraction. Hygroscopic growth measurements showed that coarse mineral dust particles can safely be treated as completely hydrophobic at least up to 85% RH. With the measured surface albedo of the bright surfaces of Southeast Morocco, the Saharan dust always had a warming effect on the atmosphere.

The regional dust model system LM-MUSCAT-DES was validated with the experimental data. Dust optical thicknesses, number size distributions and the position of the maximum dust extinction in the vertical profiles agreed well with the observations. However, the spatio-temporal evolution of the dust plumes was not always reproduced due to inaccuracies in the dust source placement by the model.

The SAMUM-1 data were also used to validate aerosol characteristics retrieved from MISR observations. Multi-angle imaging spectroradiometer mid-visible aerosol optical thickness agreed with field measurements about as well as can be expected given spatial sampling differences; the space-based observations capture aerosol trends and variability over an extended region.

With the same consortium and experimental set up, the Saharan dust plume was characterized in the far field in a follow-up experiment on the Cape Verdes in early 2008.

References

Ansmann, A., Wandinger, U., Wiedensohler, A. and Leiterer, U. 2002. Lindenberg Aerosol Characterization Experiment 1998 (LACE 98): overview. *J. Geophys. Res.* **107**, 8129, doi:8110.1029/2000JD000233.

Ansmann, A., Tesche, M., Knippertz, P., Bierwirth, E., Althausen, D. and co-authors. 2008. Vertical profiling of convective dust plumes in southern Morocco during SAMUM. *Tellus* **61B**, doi:10.1111/j.1600-0889.2008.00384.x.

Cakmur, R. V., Miller, R. L., Perlwitz, J., Geogdzhayev, I. V., Ginoux, P. and co-authors. 2006. Constraining the magnitude of the global dust cycle by minimizing the difference between a model and observations. *J. Geophys. Res.* **111**, doi:10.1029/2005JD005791.

Duce, R. A. 1995. Source, distributions and fluxes of mineral aerosols and their relationship to climate. In: *Aerosol Forcing of Climate* (eds. R. J. Charlson and J. Heintzenberg). John Wiley & Sons, New York, 43–72.

Evan, A. T., Dunion, J., Foley, J. A., Heidinger, A. K. and Velden, C. S. 2006. New evidence for a relationship between Atlantic tropical cyclone activity and African dust outbreaks. *Geophys. Res. Lett.* **33**, L19813, doi:19810.11029/12006GL026408.

Holben, B. N., Eck, T. F., Slutsker, I., Tanré, D., Buis, J. P. and co-authors. 1998. AERONET—a federated instrument network and data archive for aerosol characterization. *Remote Sens. Environ.* **66**, 1–16.

Houghton, J. T., Ding, Y., Griggs, D. J., Noguer, M., Linden, P. J. V. D. and co-authors. 2001. *Climate Change 2001: The Scientific Basis*. Cambridge University Press, Cambridge, UK.

IPCC. 2007. *Climate Change 2007: The Physical Science Basis*. Cambridge University Press, Cambridge.

Jickells, T. D., An, Z. S., Andersen, K. K., Baker, A. R., Bergametti, G. and co-authors. 2005. Global iron connections between desert dust, ocean biogeochemistry, and climate. *Science* **308**, 67–71.

Knippertz, P., Deutscher, C., Kandler, K., Müller, T., Schulz, O. and co-authors. 2007. Dust mobilization due to density currents in the Atlas region: observations from the SAMUM 2006 field campaign. *J. Geophys. Res.* **112**, doi:10.1029/2007JD008774.

Koren, I., Kaufman, Y. J., Washington, R., Todd, M. C., Rudich, Y. and co-authors. 2006. The Bodélé depression: a single spot in the Sahara that provides most of the mineral dust to the Amazonas forest. *Environ. Res. Lett.* **1**, 1–5.

Lau, K. M. and Kim, K. M. 2007. Cooling of the Atlantic by Saharan dust. *Geophys. Res. Lett.* **34**, L23811, doi:23810.21029/22007GL031538.

Liao, H. and Seinfeld, J. H. 1998. Radiative forcing by mineral dust aerosols: sensitivity to key variables. *J. Geophys. Res.* **103**, 31 637–31 645.

Myhre, G. and Stordal, F. 2001. Global sensitivity experiments of the radiative forcing due to mineral aerosols. *J. Geophys. Res.* **106**, 18 193–18 204.

Ogren, J. A. 1995. A systematic approach to *in situ* observations of aerosol properties. In: *Aerosol Forcing of Climate* (eds. R. J. Charlson and J. Heintzenberg). John Wiley & Sons, New York, 215–226.

Prospero, J. M., Ginoux, P., Torres, O., Nicholson, S. E. and Gill, T. E. 2002. Environmental characterization of global sources of atmospheric soil dust identified with the Nimbus 7 Total Ozone Mapping Spectrometer (TOMS) absorbing aerosol product. *Rev. Geophys.* **40**, doi:10.1029/2000RG000095.

Quinn, P. K., Anderson, T. L., Bates, T. S., Dlugi, R., Heintzenberg, J. and co-authors. 1996. Closure in tropospheric aerosol-climate research: a review and future needs for addressing aerosol direct shortwave radiative forcing. *Contr. Atmos. Phys.* **69**, 547–577.

Russell, P. B. and Heintzenberg, J. 2000. An overview of the ACE 2 Clear Sky Column Closure Experiment (CLEARCOLUMN). *Tellus* **52B**, 463–483.

Sokolik, I. N. and Toon, O. B. 1996. Direct radiative forcing by anthropogenic airborne mineral aerosols. *Nature* **381**, 681–683.

Sokolik, I. N., Winker, D. M., Bergametti, G., Gillette, D. A., Carmichael, G. and co-authors. 2001. Introduction to special section: outstanding problems in quantifying the radiative impacts of mineral dust. *J. Geophys. Res.* **106**, 18 015–18 027.

Tegen, I., Lacis, A. A. and Fung, I. 1996. The influence on climate forcing of mineral aerosols from disturbed soils. *Nature* **380**, 419–422.

Tegen, I., Werner, M., Harrison, S. P. and Kohfeld, K. E. 2004. Relative importance of climate and land use in determining present and future global soil dust emission. *Geophys. Res. Lett.* **31**, doi:10.1029/2003GL019216, 012004.

Wu, L. 2007. Impact of Saharan air layer on hurricane peak intensity. *Geophys. Res. Lett.* **34**, doi:10.1029/2007GL029564.